ACS APPLIED MATERIALS & INTERFACES

Research Article

www.acsami.org

Effect of Fullerene Tris-adducts on the Photovoltaic Performance of P3HT:Fullerene Ternary Blends

Hyunbum Kang,[†] Ki-Hyun Kim,[†] Tae Eui Kang,[†] Chul-Hee Cho,[†] Sunhee Park,[†] Sung Cheol Yoon,[‡] and Bumjoon J. Kim*,[†]

[†]Department of Chemical and Biomolecular Engineering, Korea Advanced Institute of Science and Technology (KAIST), Daejeon 305-701, Korea

[‡]Advanced Materials Division, Korea Research Institute of Chemical Technology (KRICT), Daejeon 305-600, Korea

Supporting Information

ABSTRACT: Fullerene tris-adducts have the potential of achieving high open-circuit voltages (V_{OC}) in bulk heterojunction (BHJ) polymer solar cells (PSCs), because their lowest unoccupied molecular orbital (LUMO) level is higher than those of fullerene mono- and bis-adducts. However, no successful examples of the use of fullerene tris-adducts as electron acceptors have been reported. Herein, we developed a ternary-blend approach for the use of fullerene tris-adducts to fully exploit the merit of their high LUMO level. The compound *o*-xylenyl C_{60} tris-adduct (OXCTA) was used as a ternary acceptor in the model system of poly(3-hexylthiophene) (P3HT) as the electron donor and the two soluble fullerene acceptors of OXCTA and fullerene monoadduct (*o*-xylenyl C_{60} monoadduct (OXCMA), phenyl C_{61}-butyric acid methyl ester (PCBM), or indene-C_{60} monoadduct (ICMA)). To explore the effect of OXCTA in ternary-blend PSC devices, the photovoltaic behavior of the device was investigated in terms of the weight fraction of OXCTA (W_{OXCTA}). When W_{OXCTA} is small (<0.3), OXCTA can generate a synergistic bridging effect between P3HT and the fullerene monoadduct, leading to simultaneous enhancement in both V_{OC} and short-circuit current (J_{SC}). For example, the ternary PSC devices of P3HT:(OXCMA:OXCTA) with W_{OXCTA} of 0.1 and 0.3 exhibited power-conversion efficiencies (PCEs) of 3.91% and 3.96%, respectively, which were significantly higher than the 3.61% provided by the P3HT:OXCMA device. Interestingly, for W_{OXCTA} > 0.7, both V_{OC} and PCE of the ternary-blend PSCs exhibited nonlinear compositional dependence on W_{OXCTA}. We noted that the nonlinear compositional trend of P3HT:(OXCMA:OXCTA) was significantly different from that of P3HT:(OXCMA:*o*-xylenyl C_{60} bis-adduct (OXCBA)) ternary-blend PSC devices. The fundamental reasons for the differences between the photovoltaic trends of the two different ternary-blend systems were investigated systemically by comparing their optical, electrical, and morphological properties.

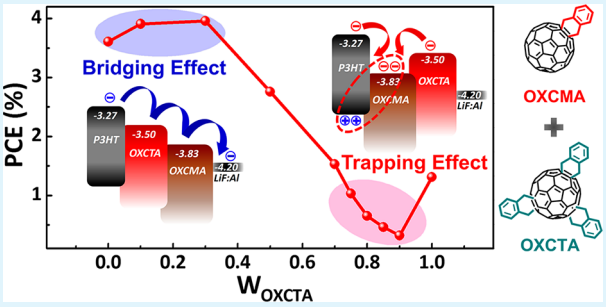

KEYWORDS: *fullerene tris-adducts, ternary-blend, polymer solar cell, bridging effect, trap-assisted recombination, charge trapping*

INTRODUCTION

Extensive research activities have been focused on developing new *p*-type low-bandgap polymers in order to increase light harvesting; these polymers produce high efficiencies in a binary blend of BHJ-type PSCs greater than 6−8%.[1−11] However, the maximized efficiency of a binary blend type polymer:fullerene BHJ PSCs theoretically is expected to be limited to 10−12%.[12] Recently, ternary-blend PSCs that consist of three active materials in a single layer have been recognized as an efficient strategy for further increasing the efficiency of the device without involving more complex design and fabrication (i.e., the tandem cell approach).[13−21] For example, a low-bandgap polymer can be incorporated into the binary P3HT:PCBM blend in order to extend its light absorption up to infrared range and increase photon harvesting, thus increasing the values of J_{SC} and PCE in ternary-blend PSCs.[16,17,22,23]

PCBM has been used extensively as a conventional fullerene acceptor, but it has a relatively low-lying LUMO level that limits the V_{OC} value of the BHJ-type PSCs. In this regard, various fullerene bis-adducts with higher LUMO levels have been designed and synthesized recently for producing high V_{OC} values in BHJ-type PSCs.[24−37] Therefore, ternary-blend PSCs based on one donor and two fullerene acceptors that have different LUMO levels could be an effective approach for optimizing V_{OC} and, consequently, the PCE in PSCs.[38−40] For example, Thompson and co-workers recently reported that the value of V_{OC} can be tuned in a ternary-blend of P3HT:PCBM:indene-C_{60} bis-adducts (ICBA) largely by varying the composition ratio between PCBM and ICBA.[38,40] However, the study of ternary-blend PSCs based

Received: February 24, 2013
Accepted: April 10, 2013
Published: April 10, 2013

   dx.doi.org/10.1021/am400695e | ACS Appl. Mater. Interfaces 2013, 5, 4401−4408

Scheme 1. Schematic Illustration of Ternary-Blend BHJ PSCs Used in This Study; Two Different Series of P3HT:(OXCMA:OXCTA) and P3HT:(OXCMA:OXCBA) were Used for the Active Layer in the PSCs

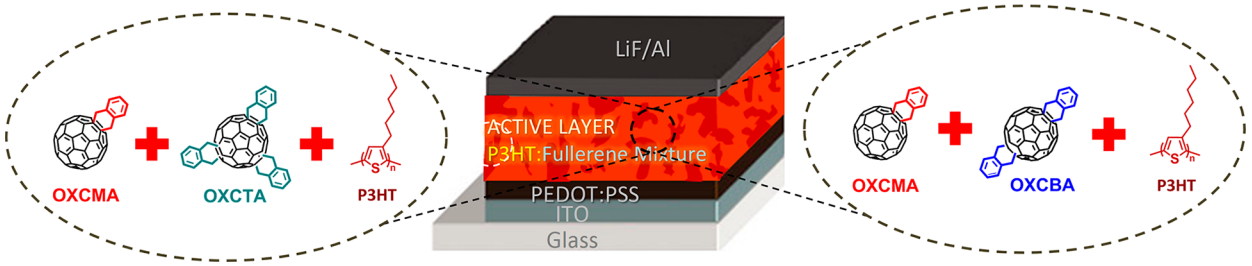

Table 1. Photovoltaic Properties of P3HT:(OXCMA:OXCTA) under AM 1.5G-Simulated Solar Illumination (100 mW cm^{-2})

P3HT:OXCMA:OXCTA (w/w/w)	OXCTA fraction in fullerene (W_{OXCTA})	V_{OC} (V)	J_{SC} (mA cm^{-2})	FF	PCE (%)
1:0.6:0	0	0.634	9.59	0.59	3.61
1:0.54:0.06	0.1	0.657	9.65	0.62	3.91
1:0.42:0.18	0.3	0.674	10.34	0.57	3.96
1:0.30:0.30	0.5	0.690	8.34	0.48	2.76
1:0.18:0.42	0.7	0.675	6.40	0.36	1.53
1:0.15:0.45	0.75	0.659	4.73	0.33	1.03
1:0.12:0.48	0.8	0.626	3.53	0.30	0.65
1:0.09:0.51	0.85	0.590	2.75	0.28	0.46
1:0.06:0.54	0.9	0.616	1.85	0.28	0.32
1:0:0.6	1.0	0.899	4.47	0.33	1.31

on two different fullerene acceptors has been very limited and a vast number of fundamental questions remain to be answered.[39] Fullerene tris-adducts, including three solubilizing groups onto a fullerene core, are interesting materials because their LUMO level is even greater than the level of fullerene bis-adducts. However, despite their potential for further enhancing the V_{OC} values in the PSCs, the binary BHJ PSC based on fullerene tris-adducts as a single-component electron acceptor had low J_{SC} and fill-factor (FF) values. They suffered from low electron mobility because of the presence of many regio-isomers, which hampers fullerene crystallization.[26,30,32,41−43]

Herein, we develop a ternary-blend approach for the use of fullerene tris-adducts to fully exploit their high LUMO levels while avoiding adverse influence on electron mobility. The fullerene tris-adduct, OXCTA, was used as a ternary acceptor in a system that consisted of P3HT and two soluble fullerene acceptors of OXCTA and fullerene monoadduct (Scheme 1). Three different fullerene monoadducts of OXCMA, PCBM, and ICMA were used to demonstrate the generality of this ternary-blend approach. When a small amount of OXCTA was incorporated into the P3HT:OXCMA binary blend, the OXCTA can enhance the V_{OC} in a ternary device and, at the same time, facilitate charge separation and transfer at the P3HT/fullerene interface. For instance, the ternary-blend PSC device at W_{OXCTA} = 0.3 had a PCE of approximately 4%, exceeding the PCEs of the corresponding P3HT:OXCMA and P3HT:OXCTA binary blends, i.e., 3.61 and 1.31%, respectively. Therefore, for the first time, we report a successful example of using fullerene tris-adducts in BHJ PSCs. In contrast, the performance of P3HT:(OXCMA:OXCTA) ternary-blend PSCs is even lower than that of the P3HT:OXCTA binary device when OXCTA is the major fullerene component in the ternary device, i.e., W_{OXCTA} > 0.7, which indicates that there is a nonlinear compositional dependence on W_{OXCTA}. As a control ternary-blend system, we fabricated P3HT:(OXCMA:OXCBA) (OXCBA, a ternary acceptor) devices that had almost linear trends of photovoltaic parameters in terms of W_{OXCBA}. To gain direct evidence of differences in the photovoltaic trends between the two types of ternary devices, we measured external quantum efficiency (EQE), internal quantum efficiency (IQE), space charge limited current (SCLC) charge mobility, and light intensity-dependent V_{OC} in terms of W_{OXCTA} or W_{OXCBA}.

RESULTS AND DISCUSSION

To investigate the effect of the fullerene tris-adducts on the photovoltaic performance of the ternary-blend PSCs, OXCTA was used as a ternary acceptor in the BHJ PSCs of P3HT and two fullerene acceptors composed of OXCTA and fullerene monoadduct. Three different series of ternary PSCs ((1) P3HT:(OXCMA:OXCTA), (2) P3HT:(ICMA:OXCTA), and (3) P3HT:(PCBM:OXCTA)) were fabricated with various weight fractions of OXCTA ranging from 0 and 1. W_{OXCTA} is the weight fraction of OXCTA to OXCTA:fullerene monoadduct in the device. Each normal-type PSC was fabricated with stack order ITO/PEDOT:PSS/P3HT:(fullerene monoadduct:OXCTA)/LiF:Al. And all the ternary devices were prepared under identical conditions, including the 100−120 nm thickness of the BHJ active layer (spuncast from 15 mg/mL P3HT in the ternary-blend solution). The overall ratio of the P3HT:fullerene mixture (1:0.6 for P3HT:(OXCMA:OXCTA) and P3HT:(ICMA:OXCTA) and 1:0.7 for P3HT:(PCBM:OXCTA)) was used to optimize each different series of the ternary-blend PSCs. Table 1 and Table S1 in the Supporting Information summarize the optimized average values of the photovoltaic characteristics (V_{OC}, J_{SC}, FF, and PCE) of the ternary-blend PSC devices measured at AM. 1.5 illumination condition. Table 1 lists the device parameters of the P3HT:(OXCMA:OXCTA) ternary-blend PSCs as a function of W_{OXCTA}. First, the PCEs of two reference devices of P3HT:OXCMA and P3HT:OXCTA blends were 3.61% (V_{OC}, 0.634 V; J_{SC}, 9.59 mA cm^{-2}; and FF, 0.59) and 1.31% (V_{OC}, 0.899 V; J_{SC}, 4.47 mA cm^{-2}; and FF, 0.33), respectively, which agrees well with our previously reported

Table 2. Characteristics of Ternary-Blend BHJ PSCs Based on P3HT:(OXCMA:OXCBA) (1:0.6 weight ratio, AM 1.5G illumination conditions)

P3HT:OXCMA:OXCBA (w/w/w)	OXCBA fraction in fullerene (W_{OXCBA})	V_{OC} (V)	J_{SC} (mA cm^{-2})	FF	PCE (%)
1:0.6:0	0	0.634	9.59	0.59	3.61
1:0.54:0.06	0.1	0.639	10.46	0.59	3.94
1:0.42:0.18	0.3	0.665	10.60	0.58	4.03
1:0.30:0.30	0.5	0.680	10.30	0.54	3.79
1:0.18:0.42	0.7	0.705	10.19	0.51	3.69
1:0.06:0.54	0.9	0.765	10.29	0.52	4.11
1:0:0.6	1.0	0.843	10.32	0.58	5.06

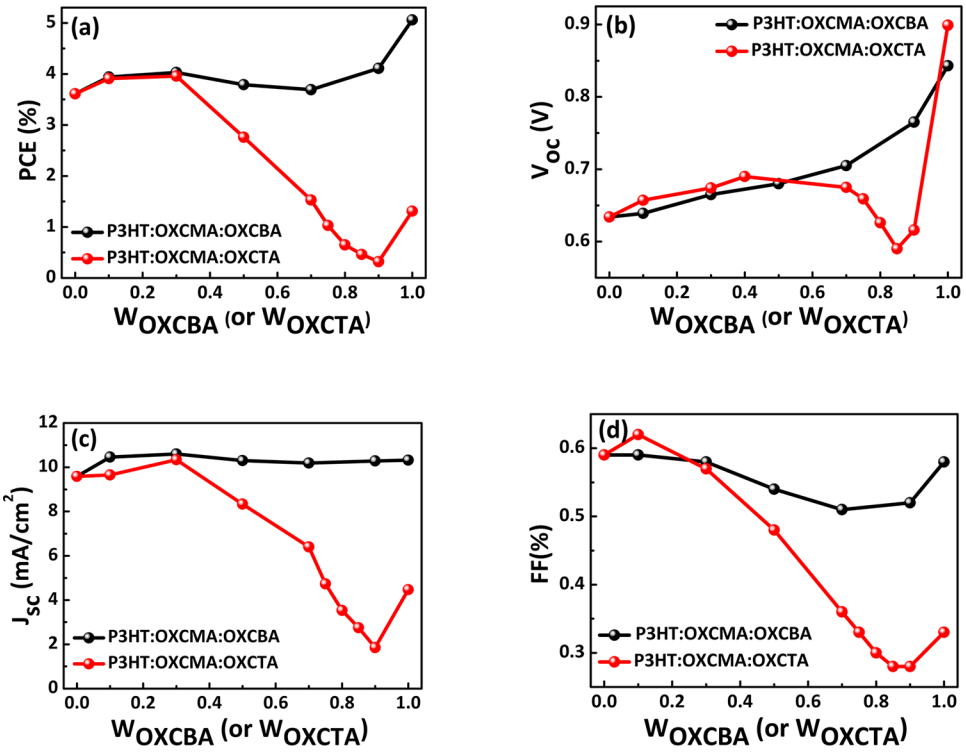

Figure 1. Variation of photovoltaic parameters ((a) PCE, (b) V_{OC}, (c) J_{SC}, and (d) FF) as a function of the W_{OXCBA} or W_{OXCTA} in ternary-blend PSC devices.

values.[30] Despite the high V_{OC} value of 0.9 V, the P3HT:OXCTA blend device had a low PCE value with low J_{SC} and FF. However, when OXCTA was added as the ternary acceptor in the P3HT:OXCMA blend, a higher PCE value of the P3HT:(OXCMA:OXCTA) was observed. As the OXCTA component increased up to W_{OXCTA} of approximately 0.3, the PCEs of the ternary devices increased noticeably by 8.3% and 9.7%, going from 3.61% with P3HT:OXCMA at W_{OXCTA}= 0 to 3.91% and 3.96% with P3HT:(OXCMA:OXCTA) at W_{OXCTA} = 0.1 and 0.3, respectively. Because of the higher LUMO level of OXCTA, at W_{OXCTA} = 0.3, the V_{OC} value increased from 0.634 to 0.674 V and, at the same time, the J_{SC} value increased from 9.59 to 10.34 mA cm^{-2}. Thus, the OXCTA ternary acceptor (W_{OXCTA} = 0.1−0.3) produced a synergistic effect by bridging the P3HT and OXCMA domains.[21,23]

When the W_{OXCTA} values were over 0.3, there was a striking difference in the photovoltaic trend of the P3HT:(OXCMA:OXCTA) devices in terms of W_{OXCTA}. As the W_{OXCTA} was increased further, the PCE of the ternary devices decreased significantly, from 3.96% (W_{OXCTA}= 0.3) to 1.31% (W_{OXCTA}= 1.0). Interestingly, the PCEs of the ternary devices in the range of W_{OXCTA}= 0.75−0.9 were even lower than that of the P3HT:OXCTA binary device. For example, the PCE of the device at W_{OXCTA}= 0.9 was only one-fourth compared to that of the P3HT:OXCTA device. Consequently, it brings out the nonlinear compositional dependence of the ternary device parameters (V_{OC}, J_{SC}, FF, and PCE) on W_{OXCTA}. The photovoltaic performances of P3HT:(ICMA:OXCTA) (see Table S1a in the Supporting Information) and P3HT:(PCBM:OXCTA) (see Table S1b in the Supporting Information) ternary-blend PSCs were also measured and compared. In both systems, the photovoltaic parameters had nonlinear compositional dependence on W_{OXCTA}, which demonstrated the generality of the photovoltaic trends of P3HT:(fullerene monoadduct:OXCTA) ternary blends as a function of W_{OXCTA}.

As a control ternary-blend system, a series of P3HT:(OXCMA:OXCBA) ternary-blend PSCs were fabricated using OXCBA as an alternative ternary acceptor, and their photovoltaic performances are summarized in Table 2. Also, the essential device parameters (V_{OC}, J_{SC}, FF, and PCE) of the P3HT:(OXCMA:OXCTA) and P3HT:(OXCMA:OXCBA) ternary-blend PSC devices are compared in Figure 1a−d. The PCE of the binary P3HT:OXCBA device was 5.06%, which agrees well with our previously reported value.[30] It is important to note that, in

contrast to the nonlinear compositional dependence of the P3HT:(OXCMA:OXCTA) ternary devices, all of the P3HT:(OXCMA:OXCBA) ternary-blend PSCs had high J_{SC} values, exceeding 10.20 mA cm^{-2} (Figure 1c), and high FF values (Figure 1d) for the entire range of W_{OXCBA} from 0 to 1. In addition, as the W_{OXCBA} increased, the V_{OC} of the P3HT:(OXCMA:OXCBA) ternary devices showed a continuous increase from 0.634 to 0.843 V (Figure 1b). This trend was consistent with that of the P3HT:(PCBM:ICBA) ternary-blend system reported by other groups.[38] The electrical, optical, and morphological properties of both the P3HT:(OXCMA:OXCTA) and P3HT:(OXCMA:OXCBA) ternary blends are discussed in detail below to elucidate the reasons that the P3HT:(OXCMA:OXCTA) devices have a nonlinear compositional dependence on W_{OXCTA}.

Light absorption in the active layer is one of the major factors that affects the J_{SC} values of PSC devices. Accordingly, thin-film UV−vis absorption spectra of both the P3HT:(OXCMA:OXCTA) and P3HT:(OXCMA:OXCBA) ternary blends were measured under optimized device conditions (Figure 2). The

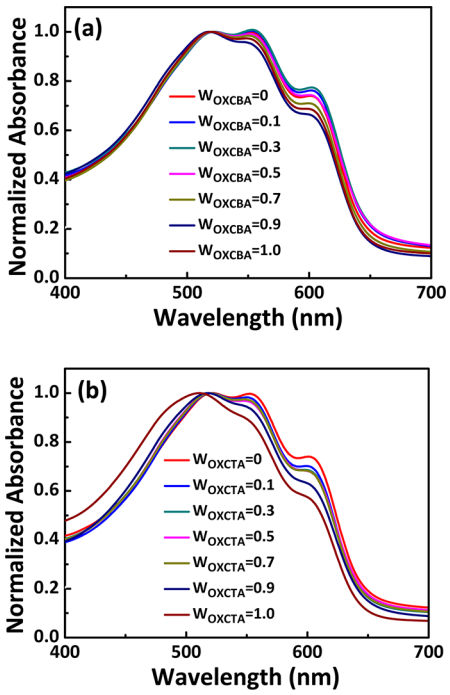

Figure 2. UV−vis absorption spectra of (a) P3HT:(OXCMA:OXCBA) and (b) P3HT:(OXCMA:OXCTA) ternary-blend films in terms of W_{OXCBA} and W_{OXCTA}. The ternary-blend films were prepared identically at optimized device conditions.

absorption spectra of all ternary-blend films displayed three maxima in the 500−600 nm range. Among the three maxima absorption peaks, the most important feature of the thin-film absorption spectra is the presence of the strong vibronic feature at ∼600 nm, which is indicative of a high degree of P3HT interchain ordering.[32] The relative intensities of the λ_{second} peak at ∼550 nm (I_{second}/I_{first}) and the vibronic peak (I_{vib}/I_{first}) at ∼600 nm compared to the first absorption peak at ∼520 nm for all of the ternary blend films were calculated, and the results are summarized in Table S2 in the Supporting Information. The absorption spectra of P3HT:OXCBA had slightly reduced values of I_{second}/I_{first} and I_{vib}/I_{first} compared to P3HT:OXCMA, but the differences were negligible. And the P3HT:OXCTA film showed a significant change in the location of the first absorption peak, with a strong hypsochromic shift (λ_{max} = 511 nm) and a reduced value of I_{vib}/I_{first} (= 0.57) compared to P3HT:OXCMA.[32] However, the optical properties of the P3HT:(OXCMA:OXCTA) device were almost independent of W_{OXCTA} up to 0.9. For example, the λ_{max}, I_{second}/I_{first}, and I_{vib}/I_{first} values of the P3HT:(OXCMA:OXCTA) ternary device with W_{OXCTA}= 0.7 were 519, 0.97, and 0.68, respectively, which were identical to the values of the highly performing P3HT:OXCBA device. The photoluminescence (PL) of the P3HT:(OXCMA:OXCTA) and P3HT:(OXCMA:OXCBA) ternary-blend films were measured with an excitation wavelength of 430 nm (see Figure S1 and Table S3 in the Supporting Information). The PL quenching efficiencies in all of the P3HT:(OXCMA:OXCBA) and P3HT:(OXCMA:OXCTA) ternary-blend films were in the range of 87−89%, relative to pristine P3HT. Therefore, the optical and morphological properties cannot explain the nonlinear compositional dependence of the performance of the P3HT:(OXCMA:OXCTA) ternary-blend PSCs.[44,45]

EQE and IQE values were measured to evaluate the spectral responses of the P3HT:(OXCMA:OXCTA) and P3HT:(OXCMA:OXCBA) PSCs. The IQE spectra, which can be obtained by dividing the EQE values by the light absorption intensities of the blend films, provide information on the components that are primarily responsible for converting the absorbed photons to collected electrons and holes.[46] As shown in Figure 3 and Figure S2 in the Supporting Information, both the maximum EQE and IQE values at W_{OXCTA}= 0.3 (58 and 67%, respectively) outperformed those of the P3HT:OXCMA blend (55 and 64%, respectively), which clearly reflected the higher J_{SC} and PCE values in the ternary PSCs at W_{OXCTA} = 0.3. On the other hand, the maximum EQE and IQE values (35 and 43%, respectively) at W_{OXCTA} = 0.9 were significantly lower than those

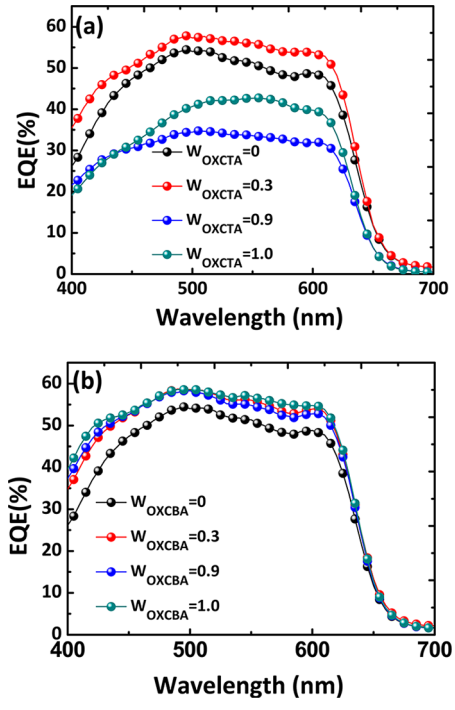

Figure 3. EQE curves of (a) P3HT:(OXCMA:OXCTA) and (b) P3HT:(OXCMA:OXCBA) ternary-blend PSCs in terms of W_{OXCTA} and W_{OXCBA}. The ternary-blend films were prepared identically at optimized device conditions.

dx.doi.org/10.1021/am400695e | ACS Appl. Mater. Interfaces 2013, 5, 4401−4408

of the P3HT:OXCTA device (43 and 50%, respectively) despite their better optical absorption, including larger λ_{max}, I_{second}/I_{first}, and I_{vib}/I_{first} values at W_{OXCTA} = 0.9 compared to those at W_{OXCTA} = 1.0. In contrast to the strong dependence of the EQE and IQE values of the P3HT:(OXCMA:OXCTA) devices on W_{OXCTA}, P3HT:(OXCMA:OXCBA) ternary-blend PSCs exhibited similar EQE and IQE values that were independent of W_{OXCBA}. The combined results of UV−vis absorption, PL quenching, and EQE measurements suggested that the difference in the electrical properties, such as the charge transfer and transport, could be the main reason for the completely different photovoltaic response in terms of W_{OXCBA} (or W_{OXCTA}) between the two different series of the ternary blends.[47−49]

To examine this possibility, we measured and compared the SCLC charge mobilities of both hole and electron-only devices of the P3HT:(OXCMA:OXCTA) and P3HT:(OXCMA:OXCBA) ternary blends. Hole and electron-only devices were constructed at optimized device conditions, with the structure of ITO/PEDOT:PSS/ternary-blends/Au and ITO/ZnO/ternary-blends/LiF:Al, respectively. Figure S3 and Table S4 in the Supporting Information show that the measured hole mobilities of all of the ternary blends were approximately the same, i.e., on the order of 1×10^{-4} cm^2/(V s) regardless of the types of ternary acceptors.[30,32] In contrast, there were significant differences in the electron mobilites between the P3HT:(OXCMA:OXCBA) and P3HT:(OXCMA:OXCTA) ternary-blend samples, as shown in Figure S4 and Table S5 in the Supporting Information. The electron mobilities of all of the P3HT:(OXCMA:OXCBA) ternary blends were in the range of 1×10^{-5} to 1×10^{-4} cm^2/(V s), showing well-balanced electron and hole mobilities. In contrast, the electron mobility of the P3HT:(OXCMA:OXCTA) ternary blends dramatically decreased by 3 orders of magnitude, from 2.78×10^{-4} cm^2/(V s) at W_{OXCTA}= 0 to 4.10×10^{-7} cm^2/(V s) at W_{OXCTA}= 1.0. Figure 4 compares the electron mobilities of

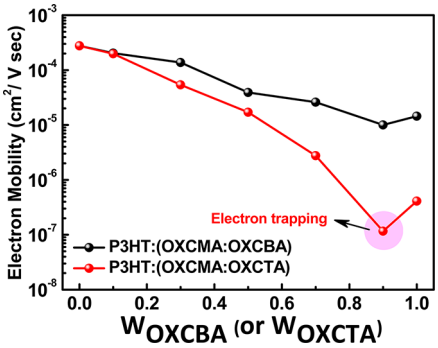

Figure 4. Variation in electron mobilties calculated by the SCLC method as a function of W_{OXCBA} and W_{OXCTA} in electron-only devices.

P3HT:(OXCMA:OXCBA) and P3HT:(OXCMA:OXCTA) in terms of W_{OXCBA} and W_{OXCTA}. It was clearly seen that the electron mobilities of the P3HT:(OXCMA:OXCTA) ternary blends in the range of W_{OXCTA}= 0.7−1.0 decreased nonlinearly as their PCE trends (decreasing order: W_{OXCTA}= 0.5, 0.7, 1.0, and 0.9). For example, the electron mobility (1.16×10^{-7} cm^2/(V s)) of the device at W_{OXCTA}= 0.9 was four times lower than that at W_{OXCTA} = 1.0. Therefore, although the OXCMA, itself, can be efficient fullerene acceptor in binary-type polymer:fullerene BHJ solar cells,[50,51] the presence of OXCMA in the OXCTA-dominant fullerene phase had an adverse impact on electron mobility and the device performance of the ternary-blend PSC devices.

Figure 5 illustrates the energy-bandgap alignment of the materials used in the ternary-blend PSCs in our system. Two different bridging and trapping effects of W_{OXCTA} on the performance of the P3HT:(OXCMA:OXCTA) PSCs were observed to be dependent on the W_{OXCTA} values: (a) bridging effect of OXCTA for the case of W_{OXCTA}= 0.1−0.3 and (b) trapping effect by OXCMA for W_{OXCTA}= 0.7−0.9. For the case in which OXCMA was used as the additive in the ternary blend (W_{OXCTA}= 0.7−0.9), OXCMA can act as charge-trapping sites in the OXCTA-dominant fullerene phase due to the significantly unmatched LUMO levels (about 0.33 eV) between OXCMA and OXCTA.[52] The presence of electron traps could give rise to immobilized electrons, which leads to highly unbalanced charge transport. As a result, trap-assisted recombination loss via combination of trap electrons and free holes can occur.[52−56] In contrast, when OXCTA was used as the additive in the ternary blend (W_{OXCTA} = 0.1−0.3), OXCTA can produce a synergistic effect on the device by bridging the P3HT and OXCMA domains, as shown in Figure 5a. OXCTA molecules can enhance the V_{OC} in the ternary device and, at the same time, promote charge transfer at the P3HT/fullerene interface. Therefore, we believe that the change in the electrical properties of the P3HT:(OXCMA:OXCTA) ternary blend driven by two different bridging and trapping effects of W_{OXCTA} was mainly responsible for the nonlinear compositional dependence of the device performance on W_{OXCTA}.

A deeper insight into the effect of W_{OXCBA} or W_{OXCTA} on the performance of the device can be obtained by measuring the dependence of the V_{OC} on light intensity, which determines the degree of electron trapping and trap-assisted electron−hole recombination. At open-circuit condition, all of the photogenerated charge carriers recombined because there was no current extraction. Therefore, at this condition, the photovoltaic parameters of a solar cell are strongly influenced by the recombination process.[54,55,57] It is well-known that the V_{OC} values of the PSCs depend on the natural logarithm of the light intensity with a slope (S) with units of k_BT/q (where k_B is the Boltzmann constant, T is temperature, and q is the elementary charge). Thus, the magnitude of the slope S depends on the strength of the charge recombination.[57] Figure 6 shows the dependence of V_{OC} on light intensity for two different series of P3HT:(OXCMA:OXCBA) and P3HT:(OXCMA:OXCTA) at different W_{OXCBA} or W_{OXCTA} values. The P3HT:(OXCMA:OXCBA) ternary-blend PSCs had similar values of S = 1.1−1.2 for the entire W_{OXCBA} range, which explained the trend of high J_{SC} and FF values in the PSCs that are independent of W_{OXCBA}. In contrast, there were striking differences in the effect of W_{OXCBA} and W_{OXCTA} on the slope S between two ternary blends. The P3HT:(OXCMA:OXCTA) devices at W_{OXCTA}= 0.3 exhibited a similar value of S = 1.19 ± 0.05 as that at W_{OXCTA}= 0 (S = 1.25 ± 0.05), but the presence of OXCMA in the OXCTA-dominant fullerene phase induced significant increase in the slope values (i.e., at W_{OXCTA} = 0.9, S= 3.22 ± 0.25). First, our results agreed well with the previous finding that binary-type polymer:fullerene solar cells based on fullerene tris-adducts had a larger dependence of the V_{OC} on light intensity than those of mono- and bis-adducts fullerene.[26] More importantly, the S value at W_{OXCTA} = 0.9 was even 46% higher than that of the P3HT:OXCTA blend (S = 2.21 ± 0.17). The strong dependence of V_{OC} on light intensity (large S) indicated the presence of electrons in the trap level, thus trap-assisted recombination was

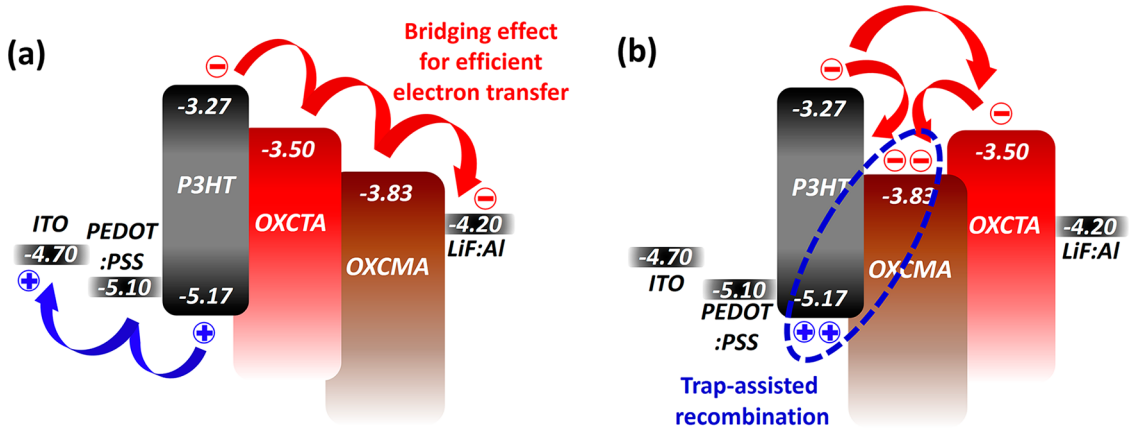

Figure 5. Energy levels (eV) of electrodes and materials used in our ternary-blend PSC system. The LUMO levels of the fullerene multiadducts (OXCMA: −3.83 eV, OXCBA: −3.66 eV, and OXCTA: −3.50 eV) were estimated by CV measurements. Two different bridging and trapping effects on the performance of the P3HT:(OXCMA:OXCTA) PSCs were observed to be dependent on the W_{OXCTA} values: (a) bridging effect of OXCTA for the case of W_{OXCTA} = 0.1−0.3 and (b) trapping effect by OXCMA for W_{OXCTA} = 0.7−0.9.

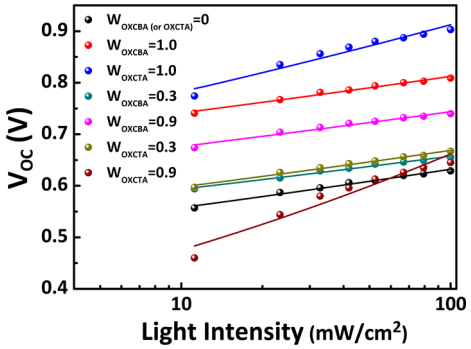

Figure 6. V_{OC} values of various ternary-blend PSCs measured at different light intensities. The slopes S of the V_{OC} vs light intensity in units of $[kT/q]$ for P3HT:(OXCMA:OXCBA) were determined: S = 1.25 ± 0.05 (W_{OXCBA} = 0); S = 1.08 ± 0.05 (W_{OXCBA} = 0.3); S = 1.14 ± 0.07 (W_{OXCBA} = 0.9); S = 1.19 ± 0.05 (W_{OXCBA} = 1). In contrast, the S values for P3HT:(OXCMA:OXCTA) were strongly dependent on W_{OXCTA}: S = 1.25 ± 0.05 (W_{OXCTA} = 0); S = 1.19 ± 0.05 (W_{OXCTA} = 0.3); S= 3.22 ± 0.25 (W_{OXCTA} = 0.9); S = 2.21 ± 0.17 (W_{OXCTA} = 1).

dominant over Langevin recombination.[54] Therefore, as shown in Figure 5b, because the LUMO level of OXCMA (−3.83 eV) was much lower than that of OXCTA (−3.50 eV), the electrons in the P3HT:(OXCMA:OXCTA) that were trapped by the addition of OXCMA promoted trap-assisted recombination, which limited the J_{SC} and FF values of the PSCs. Similar effects were reported by other groups using MDMO-PPV:PCBM:TCNQ[55] and PCDTBT:PC_{61}BM:PC_{84}BM[52,53,58,59] systems. In other words, the nonlinear compositional dependence of the photovoltaic behaviors and electron mobilities in the range of W_{OXCTA}= 0.7−1.0 was caused mainly by the presence of the charge-trapping sites of OXCMA.

Further evidence of the electron trapping effect of OXCMA in two different series of P3HT:(OXCMA:OXCBA) and P3HT:(OXCMA:OXCTA) ternary-blend PSCs were obtained by investigating the values of saturation current density (J_0). Because J_0 is a measure of "leakage" of charge carriers across the P−N junction, which induces the nonideality of the diode, it could provide useful information about the degree of the defect states at the P3HT:fullerene interface.[45,60−62] Table 3 summarizes the J_0 values that were measured for different P3HT:(OXCMA:OXCBA) and P3HT:(OXCMA:OXCTA) ternary

Table 3. Calculated J_0 Values from the *y*-Intercept of Log Plots of the Dark Current Density against Applied Voltage in the P3HT:(OXCMA:OXCBA) and P3HT:(OXCMA:OXCTA) Ternary-blend PSCs

P3HT: (OXCMA:OXCBA)	J_0 (mA cm^{-2})	P3HT: (OXCMA:OXCTA)	J_0 (mA cm^{-2})
W_{OXCBA} = 0	4.0 × 10^{-6}	W_{OXCTA}= 0	4.0 × 10^{-6}
W_{OXCBA} = 0.3	5.6 × 10^{-6}	W_{OXCTA}= 0.3	6.9 × 10^{-6}
W_{OXCBA} = 0.7	5.3 × 10^{-6}	W_{OXCTA}= 0.7	1.1 × 10^{-4}
W_{OXCBA} = 0.9	3.9 × 10^{-6}	W_{OXCTA}= 0.9	9.8 × 10^{-4}
W_{OXCBA} = 1.0	3.3 × 10^{-6}	W_{OXCTA}= 1.0	4.2 × 10^{-4}

blends. Each J_0 value was determined from the *y*-intercept of log plots of the dark current density against applied voltage curves (see Figure S5 in the Supporting Information).[53,60,61,63] The P3HT:(OXCMA:OXCBA) ternary-blend PSCs for the entire W_{OXCBA} range had similar J_0 values on the order of 1 × 10^{-6}. Therefore, the possibility of OXCMA acting as charge-trapping sites in the OXCBA-dominant fullerene phase should be low. In contrast, for a series of the P3HT:(OXCMA:OXCTA) ternary-blend PSCs, each sample had significantly different J_0 values. The P3HT:(OXCMA:OXCTA) devices at W_{OXCTA} = 0 and 0.3 had J_0 values of 4.0 × 10^{-6} and 6.9 × 10^{-6}, respectively, which are similar to those of the P3HT:(OXCMA:OXCBA) PSCs. In contrast, the J_0 values was dramatically increased by 2 orders of magnitude when W_{OXCTA} is higher than 0.7. Among them, the device at W_{OXCTA} = 0.9 exhibited the highest J_0 value of 9.8 × 10^{-4} and, thus, the highest defect sites in the device. Therefore, the trend of measured J_0 values was in excellent agreement with the trends of the electron mobility as well as the light intensity-dependent V_{OC} values in both types of ternary-blend PSCs.

CONCLUSIONS

We investigated the effect of the fullerene tris-adduct, OXCTA as a ternary acceptor on the photovoltaic behaviors of P3HT:(fullerene monoadduct:OXCTA). OXCTA additives can enhance the V_{OC} and PCE values in the P3HT:(OXCMA:OXCTA) ternary device by producing synergistic bridges between the P3HT and OXCMA domains. For example, the device at W_{OXCTA} = 0.3 showed 4% in PCE, which was about 10% increase compared to that of the P3HT:OXCMA reference device. To the best of our knowledge, our ternary-blend approach is the first

successful example for the use of the fullerene tris-adducts in PSCs. For the range of W_{OXCTA} = 0.7−1.0, there was a striking difference in the photovoltaic trend of the P3HT:(OXCMA:OXCTA) devices in terms of W_{OXCTA}. P3HT:(OXCMA:OXCTA) ternary-blend PSCs had a nonlinear compositional dependence of the photovoltaic trends in contrast to those of P3HT:(OXCMA:OXCBA) ternary-blend PSCs. OXCMA additives act as charge-trapping sites in the P3HT:(OXCMA:OXCTA), thus preventing efficient charge transport and promoting trap-assisted recombination, as evidenced by the dramatic decrease in the SCLC electron mobility and much stronger dependence of V_{OC} on light intensity. For example, the electron mobility at W_{OXCTA} = 0.9 was four times lower than that at W_{OXCTA} = 1.0, whereas the slope of the V_{OC} dependence on light intensity at W_{OXCTA} = 0.9 was 46% higher than that at W_{OXCTA} = 1.0. Our work provides a model system for fundamental understanding of the ternary-blend device function based on one donor-two fullerene acceptors and suggests the design rule of ternary-blend for efficient PSCs.

■ ASSOCIATED CONTENT

Supporting Information

Materials and methods, detailed experimental procedures, and additional data. This material is available free of charge via the Internet at http://pubs.acs.org.

■ AUTHOR INFORMATION

Corresponding Author

*E-mail: bumjoonkim@kaist.ac.kr.

Notes

The authors declare no competing financial interest.

■ ACKNOWLEDGMENTS

This research was supported by the National Research Foundation Grant (2011-0030387), and by the Global Frontier R&D Program on Center for Multiscale Energy System (2012M3A6A7055540), funded by the Korean Government and the Research Project of the KAIST EEWS Initiative (EEWS-N01110441). This research was also supported by the New & Renewable Energy KETEP Grant (2010-T100100460) and the Fundamental R&D Program Grant for Core Technology of Materials funded by the Ministry of Knowledge Economy, Republic of Korea. The authors thank Prof. Barry Thompson for the helpful discussions.

■ REFERENCES

(1) Chu, T. Y.; Lu, J. P.; Beaupre, S.; Zhang, Y. G.; Pouliot, J. R.; Wakim, S.; Zhou, J. Y.; Leclerc, M.; Li, Z.; Ding, J. F.; Tao, Y. *J. Am. Chem. Soc.* **2011**, *133*, 4250−4253.

(2) Piliego, C.; Holcombe, T. W.; Douglas, J. D.; Woo, C. H.; Beaujuge, P. M.; Frechet, J. M. J. *J. Am. Chem. Soc.* **2010**, *132*, 7595−7597.

(3) Price, S. C.; Stuart, A. C.; Yang, L. Q.; Zhou, H. X.; You, W. *J. Am. Chem. Soc.* **2011**, *133*, 4625−4631.

(4) Zhou, H. X.; Yang, L. Q.; Stuart, A. C.; Price, S. C.; Liu, S. B.; You, W. *Angew. Chem., Int. Ed.* **2011**, *50*, 2995−2998.

(5) Ong, K. H.; Lim, S. L.; Tan, H. S.; Wong, H. K.; Li, J.; Ma, Z.; Moh, L. C. H.; Lim, S. H.; De Mello, J. C.; Chen, Z. K. *Adv. Mater.* **2011**, *23*, 1409−1413.

(6) Huo, L. J.; Zhang, S. Q.; Guo, X.; Xu, F.; Li, Y. F.; Hou, J. H. *Angew. Chem., Int. Ed.* **2011**, *50*, 9697−9702.

(7) Liang, Y. Y.; Feng, D. Q.; Wu, Y.; Tsai, S. T.; Li, G.; Ray, C.; Yu, L. P. *J. Am. Chem. Soc.* **2009**, *131*, 7792−7799.

(8) Li, Y. F. *Acc. Chem. Res.* **2012**, *45*, 723−733.

(9) Small, C. E.; Chen, S.; Subbiah, J.; Amb, C. M.; Tsang, S. W.; Lai, T. H.; Reynolds, J. R.; So, F. *Nat. Photonics* **2012**, *6*, 115−120.

(10) He, Z. C.; Zhong, C. M.; Huang, X.; Wong, W. Y.; Wu, H. B.; Chen, L. W.; Su, S. J.; Cao, Y. *Adv. Mater.* **2011**, *23*, 4636−4643.

(11) Green, M. A.; Emery, K.; Hishikawa, Y.; Warta, W.; Dunlop, E. D. *Prog. Photovolt.: Res. Appl.* **2011**, *19*, 565−572.

(12) Scharber, M. C.; Wuhlbacher, D.; Koppe, M.; Denk, P.; Waldauf, C.; Heeger, A. J.; Brabec, C. L. *Adv. Mater.* **2006**, *18*, 789−794.

(13) Thompson, B. C.; Kim, Y. G.; Reynolds, J. R. *Macromolecules* **2005**, *38*, 5359−5362.

(14) Yang, L. Q.; Zhou, H. X.; Price, S. C.; You, W. *J. Am. Chem. Soc.* **2012**, *134*, 5432−5435.

(15) Chen, C. H.; Hsieh, C. H.; Dubosc, M.; Cheng, Y. J.; Su, C. S. *Macromolecules* **2010**, *43*, 697−708.

(16) Koppe, M.; Egelhaaf, H. J.; Dennler, G.; Scharber, M. C.; Brabec, C. J.; Schilinsky, P.; Hoth, C. N. *Adv. Funct. Mater.* **2010**, *20*, 338−346.

(17) Khlyabich, P. P.; Burkhart, B.; Thompson, B. C. *J. Am. Chem. Soc.* **2012**, *134*, 9074−9077.

(18) Adam, G.; Pivrikas, A.; Ramil, A. M.; Tadesse, S.; Yohannes, T.; Sariciftci, N. S.; Egbe, D. A. M. *J. Mater. Chem.* **2011**, *21*, 2594−2600.

(19) Mikroyannidis, J. A.; Tsagkournos, D. V.; Balraju, P.; Sharma, G. D. *J. Power Sources* **2011**, *196*, 2364−2372.

(20) Chen, C. H.; Cheng, Y. J.; Dubosc, M.; Hsieh, C. H.; Chu, C. C.; Hsu, C. S. *Chem.−Asian J.* **2010**, *5*, 2483−2492.

(21) Cha, H.; Chung, D. S.; Bae, S. Y.; Lee, M.-J.; An, T. K.; Hwang, J.; Kim, K. H.; Kim, Y.-H.; Choi, D. H.; Park, C. E. *Adv. Funct. Mater.* **2013**, *23*, 1556−1565.

(22) Machui, F.; Rathgeber, S.; Li, N.; Ameri, T.; Brabec, C. J. *J. Mater. Chem.* **2012**, *22*, 15570−15577.

(23) Ameri, T.; Min, J.; Li, N.; Machui, F.; Baran, D.; Forster, M.; Schottler, K. J.; Dolfen, D.; Scherf, U.; Brabec, C. J. *Adv. Energy Mater.* **2012**, *2*, 1198−1202.

(24) Lenes, M.; Wetzelaer, G. J. A. H.; Kooistra, F. B.; Veenstra, S. C.; Hummelen, J. C.; Blom, P. W. M. *Adv. Mater.* **2008**, *20*, 2116−2119.

(25) Ross, R. B.; Cardona, C. M.; Guldi, D. M.; Sankaranarayanan, S. G.; Reese, M. O.; Kopidakis, N.; Peet, J.; Walker, B.; Bazan, G. C.; Van Keuren, E.; Holloway, B. C.; Drees, M. *Nat. Mater.* **2009**, *8*, 208−212.

(26) Lenes, M.; Shelton, S. W.; Sieval, A. B.; Kronholm, D. F.; Hummelen, J. C.; Blom, P. W. M. *Adv. Funct. Mater.* **2009**, *19*, 3002−3007.

(27) He, Y. J.; Chen, H. Y.; Hou, J. H.; Li, Y. F. *J. Am. Chem. Soc.* **2010**, *132*, 1377−1382.

(28) Zhao, G. J.; He, Y. J.; Li, Y. F. *Adv. Mater.* **2010**, *22*, 4355−4358.

(29) He, Y. J.; Zhao, G. J.; Peng, B.; Li, Y. F. *Adv. Funct. Mater.* **2010**, *20*, 3383−3389.

(30) Kim, K. H.; Kang, H.; Nam, S. Y.; Jung, J.; Kim, P. S.; Cho, C. H.; Lee, C.; Yoon, S. C.; Kim, B. J. *Chem. Mater.* **2011**, *23*, 5090−5095.

(31) Voroshazi, E.; Vasseur, K.; Aernouts, T.; Heremans, P.; Baumann, A.; Deibel, C.; Xue, X.; Herring, A. J.; Athans, A. J.; Lada, T. A.; Richter, H.; Rand, B. P. *J. Mater. Chem.* **2011**, *21*, 17345−17352.

(32) Kang, H.; Cho, C. H.; Cho, H. H.; Kang, T. E.; Kim, H. J.; Kim, K. H.; Yoon, S. C.; Kim, B. J. *ACS Appl. Mater. Interfaces* **2012**, *4*, 110−116.

(33) He, Y. J.; Li, Y. F. *Phys. Chem. Chem. Phys.* **2011**, *13*, 1970−1983.

(34) Kim, B.; Lee, J.; Seo, J. H.; Wudl, F.; Park, S. H.; Yang, C. *J. Mater. Chem.* **2012**, *22*, 22958−22963.

(35) Kim, B.; Yeom, H. R.; Choi, W. Y.; Kim, J. Y.; Yang, C. *Tetrahedron* **2012**, *68*, 6696−6700.

(36) Kang, D. J.; Kang, H.; Kim, K. H.; Kim, B. J. *ACS Nano* **2012**, *6*, 7902−7909.

(37) Cho, C. H.; Kim, H. J.; Kang, H.; Shin, T. J.; Kim, B. J. *J. Mater. Chem.* **2012**, *22*, 14236−14245.

(38) Khlyabich, P. P.; Burkhart, B.; Thompson, B. C. *J. Am. Chem. Soc.* **2011**, *133*, 14534−14537.

(39) Li, H.; Zhang, Z. G.; Li, Y. F.; Wang, J. Z. *Appl. Phys. Lett.* **2012**, *101*, 163302.

(40) Street, R. A.; Davies, D.; Khlyabich, P. P.; Burkhart, B.; Thompson, B. C. *J. Am. Chem. Soc.* **2013**, *135*, 986−989.

(41) Faist, M. A.; Keivanidis, P. E.; Foster, S.; Wobkenberg, P. H.; Anthopoulos, T. D.; Bradley, D. D. C.; Durrant, J. R.; Nelson, J. *J. Polym. Sci., Part B: Polym. Phys.* **2011**, *49*, 45−51.
(42) Guilbert, A. A. Y.; Reynolds, L. X.; Bruno, A.; MacLachlan, A.; King, S. P.; Faist, M. A.; Pires, E.; Macdonald, J. E.; Stingelin, N.; Haque, S. A.; Nelson, J. *Acs Nano* **2012**, *6*, 3868−3875.
(43) Nardes, A. M.; Ferguson, A. J.; Whitaker, J. B.; Larson, B. W.; Larsen, R. E.; Maturova, K.; Graf, P. A.; Boltalina, O. V.; Strauss, S. H.; Kopidakis, N. *Adv. Funct. Mater.* **2012**, *22*, 4115−4127.
(44) Kim, K. H.; Kang, H.; Kim, H. J.; Kim, P. S.; Yoon, S. C.; Kim, B. J. *Chem. Mater.* **2012**, *24*, 2373−2381.
(45) Yamamoto, S.; Orimo, A.; Ohkita, H.; Benten, H.; Ito, S. *Adv. Energy Mater.* **2012**, *2*, 229−237.
(46) Park, S. H.; Roy, A.; Beaupre, S.; Cho, S.; Coates, N.; Moon, J. S.; Moses, D.; Leclerc, M.; Lee, K.; Heeger, A. J. *Nat. Photonics* **2009**, *3*, 297−U295.
(47) Melzer, C.; Koop, E. J.; Mihailetchi, V. D.; Blom, P. W. M. *Adv. Funct. Mater.* **2004**, *14*, 865−870.
(48) Mihailetchi, V. D.; Xie, H. X.; de Boer, B.; Koster, L. J. A.; Blom, P. W. M. *Adv. Funct. Mater.* **2006**, *16*, 699−708.
(49) Azimi, H.; Senes, A.; Scharber, M. C.; Hingerl, K.; Brabec, C. J. *Adv. Energy Mater.* **2011**, *1*, 1162−1168.
(50) Jamieson, F. C.; Domingo, E. B.; McCarthy-Ward, T.; Heeney, M.; Stingelin, N.; Durrant, J. R. *Chem. Sci.* **2012**, *3*, 485−492.
(51) Shoaee, S.; Eng, M. P.; Espildora, E.; Delgado, J. L.; Campo, B.; Martin, N.; Vanderzande, D.; Durrant, J. R. *Energy Environ. Sci.* **2010**, *3*, 971−976.
(52) Street, R. A.; Krakaris, A.; Cowan, S. R. *Adv. Funct. Mater.* **2012**, *22*, 4608−4619.
(53) Cowan, S. R.; Leong, W. L.; Banerji, N.; Dennler, G.; Heeger, A. J. *Adv. Funct. Mater.* **2011**, *21*, 3083−3092.
(54) Mandoc, M. M.; Veurman, W.; Koster, L. J. A.; de Boer, B.; Blom, P. W. M. *Adv. Funct. Mater.* **2007**, *17*, 2167−2173.
(55) Mandoc, M. M.; Kooistra, F. B.; Hummelen, J. C.; de Boer, B.; Blom, P. W. M. *Appl. Phys. Lett.* **2007**, *91*, 263505.
(56) Kuik, M.; Koster, L. J. A.; Wetzelaer, G. A. H.; Blom, P. W. M. *Phys. Rev. Lett.* **2011**, *107*, 256805.
(57) Koster, L. J. A.; Mihailetchi, V. D.; Ramaker, R.; Blom, P. W. M. *Appl. Phys. Lett.* **2005**, *86*, 123505.
(58) Leong, W. L.; Cowan, S. R.; Heeger, A. J. *Adv. Energy Mater.* **2011**, *1*, 517−522.
(59) Kaake, L.; Dang, X.-D.; Leong, W. L.; Zhang, Y.; Heeger, A.; Nguyen, T.-Q. *Adv. Mater.* **2012**, *25*, 1706−1712.
(60) Wetzelaer, G. A. H.; Kuik, M.; Lenes, M.; Blom, P. W. M. *Appl. Phys. Lett.* **2011**, *99*, 153506.
(61) Namkoong, G.; Kong, J.; Samson, M.; Hwang, I.-W.; Lee, K. *Org. Electron.* **2013**, *14*, 74−79.
(62) Farag, A. A. M.; El-Shazly, E. A. A.; Abdel Rafea, M.; Ibrahim, A. *Sol. Energy Mater. Sol. Cells* **2009**, *93*, 1853−1859.
(63) Lee, J. H.; Cho, S.; Roy, A.; Jung, H. T.; Heeger, A. J. *Appl. Phys. Lett.* **2010**, *96*, 163303.